Actively Controlled Landing Gear For Aircraft Vibration Reduction

Lucas G. Horta, Robert H. Daugherty, and Veloria J. Martinson

Abstract

Concepts for long-range air travel are characterized by airframe designs with long, slender, relatively flexible fuselages. One aspect often overlooked is ground induced vibration of these aircraft. This paper presents an analytical and experimental study of reducing ground-induced aircraft vibration loads using actively controlled landing gears. A facility has been developed to test various active landing gear control concepts and their performance. The facility uses a NAVY A6-intruder landing gear fitted with an auxiliary hydraulic supply electronically controlled by servo valves. An analytical model of the gear is presented including modifications to actuate the gear externally and test data is used to validate the model. The control design is described and closed-loop test and analysis comparisons are presented.

1. Introduction

Long, slender, flexible fuselage configurations, especially those with a long overhang from the nose gear to the cockpit, are susceptible to ground-induced vibration problems, particularly those produced by operating over long-period, low-amplitude elevation disturbances on runways. Although in-flight vibrations are also a concern, the work discussed herein will address the mitigation of vibrations transmitted from the ground to the aircraft fuselage. The mitigation is accomplished by embedding a control system directly into the landing gear.

This paper presents results from an activity at NASA investigating three aspects of actively controlled landing gear; analytical modeling, control system design, and experimental validation. This work is aimed at improving the fidelity of analytical models to the point where they can be used for control design; experimental demonstration of various control philosophies, and to develop an experimental facility that permits development of realistic concepts that can be transitioned to commercial applications.

Development of landing gear analysis dates back to the late fifties[1,2]. Work has included numerical simulation techniques and experimental measurements to validate the various computer programs. A significant volume of the work available in the literature deals with military aircraft requiring accurate prediction of taxi loads over repaired, bomb-damaged runways [3-6]. A computer simulation program named HAVE BOUNCE[6] was developed to simulate the dynamic response of military aircraft over bomb damaged runways. To validate the computer code, model validation was performed at the Aircraft Ground Induced Loads Excitation (AGILE)[7] test facility at Wright-Patterson Air Force Base. Recently, attention has focused on ride quality during taxi, takeoff and landing[8,9]. A simulation program, developed by Stirling Dynamics[8,9], is a good example of new simulation capabilities.

Since the primary design driver in landing gear design is impact loading, landing gear are typically tuned passively for impact loading upon landing. Ross and Edson[10,11] are among the first to consider an actively controlled landing gear to reduce landing loads. Their work led to the actively control landing gear concept described in this paper. Ross and Edson demonstrated the benefits of using an actively controlled landing gear system to reduce impact loads upon landing and while traversing bombed damage runways. Work by Freymann[12] demonstrated analytically and experimentally the benefits of actively controlled landing gears in reducing landing loads and vibrations under various runway profiles. Daniels[13] presented analysis and test results for an A6 intruder landing gear system. This paper discusses an extension of the work in reference 13 to incorporate active controls. An A6-Intruder landing gear was used in the laboratory because it was readily available. Necessary modifications to the gear are described along with the facility used in the experimental validation phase.

2. Analytical Model

To extend the work by Ross and Edson[10], this research discusses an independent development of a mathematical model of a main landing gear. The nonlinear equations of motion were developed for a telescoping main gear modified with an external hydraulic system for actuation and control of the gear. Specific details of the landing gear were taken from technical drawings supplied by the Grumman Company.

Figure 1 shows a schematic of a landing gear used in the development of the equations of motion. This schematic is representative of a general telescoping-type main landing gear. The model includes the aerodynamic lift on the airplane L, the mass of the airplane's fuselage lumped with the mass of the main cylinder as M_u, and the mass of the piston lumped with the mass of the tire as M_L. The inertial position of the upper mass is X_{wg} with zero value when the gear is fully extended and the tire just touching the ground. From this same configuration X_a is the position of the lower mass taken as zero at the axle of the tire. When the gear is compressed, X_a measures the deflection of the tire to an inertial reference ground input $U(t)$. Part of the upper cylinder chamber is filled with compressed nitrogen to provide the system with a spring. The cross sectional area of the upper chamber is denoted by A_u and the corresponding pressure is P_u. Likewise, the lower chamber has cross sectional area denoted A_L and a corresponding pressure P_L. Hydraulic fluid moves between the upper and lower chamber through an orifice plate with a hole of diameter D_{op}. A tapered pin attached to the piston, known as a metering pin, is used to obstruct the flow and effectively vary the orifice diameter as the pin moves through the orifice. The pin diameter is a function of X_s and is denoted as $D_{pin}(X_s)$. Hydraulic fluid reaches the snubber chamber through several orifices of diameter D_s. In the snubber chamber, the annulus area is denoted by A_R and the pressure is P_S. The diameter of the piston is D_p. The figure denotes entry/exit ports in the upper and lower chambers for the exchange of hydraulic fluid used by the active control system. Tire spring and damping coefficients are denoted by K_t and C_t.

Figure 2 shows the forces acting on the upper mass. Balancing the forces acting on the upper mass yields the following equation:

$$\begin{aligned} M_u\ddot{X}_{wg} &= M_u g - L - P_u A_o - P_L(A_L - A_o) + P_s A_R - f \\ &= F_1 - f \end{aligned} \tag{1}$$

where F_1 is a newly defined term in Eq. (1), g is the gravitational acceleration, f is friction force between the piston and the cylinder wall, and all other terms were described previously. This equation assumes that the hydraulic fluid pressure in the upper cylinder is identical to the nitrogen pressure. Also, in this development, the variable A_o, the main orifice area, reflects the fact that the metering pin is included, i.e. it is a variable cross-sectional area depending on stroke of the piston.

Figure 3 shows the forces acting on the piston. Summing the forces on the lower mass (piston) the force balance equation is:

$$\begin{aligned} M_L\ddot{X}_a &= M_L g + P_L(A_L - A_S) - P_s(A_R - A_S) - F_t + f \\ &= F_2 + f \end{aligned} \tag{2}$$

where F_2 is a newly defined in Eq. (2). F_t is the force that is transmitted through the tire from the ground and has the form:

$$F_t = K_t(X_a + U) + C_t(\dot{X}_a + \dot{U})$$

where the tire force is defined as a linear function of tire stiffness and damping. The tire stiffness and damping coefficients are obtained by linearizing the behavior of the tire about its nominal operating point. Since all the pressures are functions of stroke, a more convenient coordinate to use is stroke. Defining the stroke coordinate as $X_s = X_{wg} - X_a$, Eqs. (1) and (2) can be written as

$$\begin{aligned} M_u \ddot{X}_{wg} &= F_1 - f \\ M_L \ddot{X}_s &= {}^{M_L}\!/_{M_u} F_1 - F_2 - (1 + {}^{M_L}\!/_{M_u}) f \end{aligned} \tag{3}$$

The discussion so far relates forces F_1 and F_2 to corresponding pressures. The pressures are functions of the displacements and velocities of the landing gear components. Details of derivations relating chamber pressures, forces, and actuation commands to landing gear motion are discussed in reference 14, but a few key expressions are included here for completeness. The expression governing hydraulic fluid flow into the landing gear system is

$$Q_c^i = -C_c x_c \sqrt{P_{High} - P_L} \qquad x_c < 0 \tag{4}$$

where Q_c^i is flow into the landing gear system, C_c is an experimentally determined orifice discharge coefficient, x_c is the control command, P_{High} is the high pressure value, and P_L is the lower chamber internal pressure. A typical expression relating pressures to stroke is

$$E_1 \sqrt{P_u - P_L} + C_c x_c \sqrt{P_{High} - P_L} = (A_L - A_R)\dot{X}_s, \quad x_c < 0 \tag{5}$$

where E_1 includes all the main orifice parameters. Equation (5) is an algebraic equation for P_L that needs to be solved for each value of $\dot{X}_s$ during the numerical simulation. In the following, a description of a general approach for control design is presented.

3. Control System Design

To control the motion of the landing gear, hydraulic fluid from auxiliary tanks is used in conjunction with electronically controlled valves to actuate the gear. The goal for control design is to minimize disturbance propagation from the ground into the fuselage. To aid the discussion on control design methodology, consider a linearized representation of the landing gear and servo valves transformed using Laplace's transform into *G(s)*. Using feedback control, as indicated in figure 4, one can design a controller *k(s)* to command the servo valves.

Define *r(s)* as an arbitrary input reference signal, *d(s)* as an unknown external disturbance, *y(s)* as the controlled response, and *m(s)* as sensor noise. After some block diagram manipulation, the controlled response is given by:

$$y(s) = (I + G(s)k(s))^{-1}\left[d(s) + G(s)k(s)r(s) - G(s)k(s)m(s)\right] \tag{4}$$

The factor $I + G(s)k(s)$ is the output return difference and multiplies every term in the right hand side of the equation. To minimize the effects of the disturbance *d(s)* on the response, the factor multiplying the disturbance term *d(s)* must be made small, i.e. the return difference must be large (i.e. $G(s)k(s) >> 1$) in the frequency range of interest. Since *G(s)* is fixed, the control designer's task is to maximize the return difference value by adjusting $k(s)$ while maintaining the stability of the system. To ensure a stable design, Nyquist criterion is used for this single-input single-output problem. Since the landing gear behavior is highly non-linear one must examine bounds of variations in the system dynamics to ensure a stable design. Nyquist criterion was computed experimentally to assess stability and gain margins of the design. Although

application of these techniques to nonlinear systems is limited, they provide tremendous insight into design philosophy and stability analysis.

4. Experimental Facility

Figure 5 shows an A6 Intruder main landing gear installed underneath a drop carriage in the standard vertical position. A connecting plate was fabricated to allow for normal mounting of the gear to the plate, and the plate was then rigidly connected to the drop carriage. The drop carriage is a truss-structure that weighs about 4.5 tons and allows unrestrained vertical motion. The drop carriage rests on the landing gear. This mass simulates the rigid portion of the aircraft mass carried by the gear. Once the gear is loaded, a shaker table is used to input forces into the gear. Hydraulic lift cylinders, powered by a hydraulic pump, are used to lift the drop carriage and unload the landing gear. Once the landing gear has been lifted, the ability exists to lock the landing gear in that position with hydraulic valves.

The hydraulic shaker table was built specifically for the task of testing landing gears. The specifications included the capability to perform a one-inch step bump in 2 milliseconds while bearing 12,000 lbm. Input waveforms such as 1-cos(x), sin(x), trapezoidal with user-selected rise time, and a saw-tooth wave-form are all accurately reproduced by the shaker table . General profiles using runway elevation versus time data are also reproduced well for low frequencies. The shaker table is capable of applying dynamic forces of up to 12,000 lbf. on the test mass and allows actuator movement of 6 inches.

The landing gear was modified in a number of ways. Two electro-hydraulic servo valves were attached to the outside of the landing gear on flat areas that had been machined on the outer cylinder of the landing gear. One valve was located above the orifice plate of the landing gear (in the upper chamber), and the other valve was located below the orifice plate (in the lower chamber). Holes were machined into the landing gear so that the valves could transfer pressurized hydraulic fluid either into or out of the desired chamber. Both valves were designed to have flow rates of at least 26 gallons per minute (gpm) at 600 PSI with a response approaching 100 Hz. A high-pressure accumulator was mounted on the upper mass (drop carriage) and kept charged to a pressure approximately twice that of the static, loaded charge pressure in the landing gear. A low-pressure accumulator was also installed so that when desired, pressurized hydraulic fluid in the landing gear could be directed there, reducing the transient back-pressure that would tend to restrict the outward flow of hydraulic fluid. The low-pressure accumulator was maintained at essentially atmospheric pressure. Ultimately, the low-pressure accumulator was attached to an atmospheric pressure reservoir where the pump used to supply the high-pressure accumulator was located. The system was thus pressure-balanced evenly around the nominal static, loaded charge pressure of the landing gear, permitting roughly equal flow rates into or out of the landing gear at similar servo command levels.

The piston head of the landing gear was also modified. Normally, a landing gear such as this has a snubber chamber that is designed to limit the speed of piston extension to prevent a significant "bottoming out" shock on the landing gear components such as might occur after a catapult during an aircraft carrier launch. Thus, normally the hydraulic damping characteristics of the landing gear vary depending on the direction of piston travel. In this experiment, it was desirable to remove the "snubber" effect so that the damping behavior was more even in both directions. To that end, a ring mounted directly under the piston head, which normally acts as a directional valve and restricts hydraulic fluid motion in one direction, was modified by drilling additional holes in it so that it provided equal flow past it regardless of the direction of hydraulic fluid motion. These changes were accurately reflected in the modeling of the landing gear for analytical purposes.

The top of the landing gear was modified slightly to accept a high-strength site glass. This site glass allowed a visual indication of the proper servicing level of hydraulic fluid prior to being pressurized with nitrogen, and saved a significant amount of time in pre-test operations.

The landing gear was instrumented to provide the necessary information for model validation. There were two accelerometers, one placed at the upper mass and the second one at the lower mass. Two relative displacement transducers were also used, one to locate the upper mass with respect to a fixed position on the carriage and one to measure the relative position between the upper and lower masses of the landing gear. Two pressure transducers were used to verify some basic model assumptions, mainly that the hydraulic fluid and the gas do not mix to any significant degree after initial shaking. One pressure transducer was located just outside the charge port of the upper cylinder, and the other was embedded in the piston head. Vertical load was inferred by measuring bending moments induced by the tire using a strain gage on the wheel axle.

5. Test Results and Model Validation

The following section discusses experimental results from tests conducted on the landing gear system. First, the servo loop dynamics and electronics were characterized and are compared with the analytical model. Second, the simulation model which was constructed using a commercially available software is described. Finally, test results for various open-loop and closed-loop cases are presented.

5.1 Numerical Solution of Equations of Motion

The fundamental equations presented in Section 2 along with key expressions discussed in Ref. 14 were programmed and numerically integrated using Simulink/Matlab[15] computer simulation program. Two types of tests were conducted as part of the analytical model validation; parameter estimation tests for characterization of the servo loop dynamics and system tests to compare overall behavior of the landing gear when operating. In the following sections test and analysis results are discussed.

5.2 Servo Loop Dynamic Characterization

Figure 6 presents a plot of hydraulic fluid flow rate as a function of servo command. These data were measured by removing nitrogen from the unrestrained landing gear and computing flow rates by measuring piston stroke rates as a result of discrete servo commands. Tests were then conducted with the piston restrained from moving to characterize the servo loop dynamics with minimum interference from piston motion. The slope of the measured flow rate versus command gives the product $C_c\sqrt{\Delta P}$, where ΔP is the pressure difference between the supply or return and the strut internal pressure. Using these results, the servo effective discharge coefficient was calculated to be $C_c = 1.0765 \times 10^{-6}$. To compare simulated chamber pressures to test, a test was conducted using a sinusoidal sweep from 0.5 Hz to 10 Hz. Input voltages from test were input into the simulation and the computed frequency response for upper chamber pressure to servo command is shown in figure 7. Test results are depicted using a solid line and simulation with a dashed line. Lower chamber tests results (not shown) are similar but with slightly more phase delay between commands and internal pressure variations. The initial pressure in the chamber was recorded as 350 PSI, the initial stroke was 10.3 inches, and the high pressure accumulator pressure was 750 PSI. The nitrogen level was estimated to be 4.78 inches. The upper curve in figure 7 shows the magnitude ratio of upper pressure to input voltage as a function of frequency, whereas the lower curve shows a phase comparison. This transfer function represents the servo valve hydraulic system response at the conditions mentioned previously.

5.3 Landing Gear Dynamic Characterization and Model Validation

Runway elevations and servo command voltages were the two inputs used to characterize the landing gear. Since the system is highly nonlinear, sine sweeps were the main form of excitation. Time simulations were performed using Simulink.

Since the simulation is nonlinear, initial conditions for the different parameters have to be set properly or time integration will fail. Conditions such as upper mass position and velocity, piston stroke, stroke rate, upper chamber pressure, and nitrogen level must all be specified. In the initial design, two sensors were used to control the motion of the landing gear; piston stroke and upper mass acceleration. Since the axle load signal from the strain gage is proportional to the upper mass acceleration, the strain gage output was used for later tests. The axle-mounted strain gages had the additional benefit of being relatively "quiet" and avoided the more dynamic nature of acceleration measurements on stiff structures such as those observed using the upper mass accelerometer.

The controller used for all the closed-loop tests was synthesized with the aid of an experimentally determined Nyquist diagram. To compensate for phase lag of the servo valves and hydraulic system, a lead-lag compensator was used to add about 10 degrees of lead at 1.5 Hz. Direct axle load feedback with a loop gain of 1 volt/6731 lbf. was used for all the closed-loop test results shown.

Shaker head position, servo-input command, piston position, upper mass position, internal pressures, and acceleration responses are compared to simulation results in figure 8. Solid lines correspond to test and dashed lines are simulation results. The input runway elevation is a sinusoid with amplitude of 0.75 inches at a frequency of 1.5 Hz. Piston position feedback is always used to maintain inter-chamber leakage through the servo valve from depleting the hydraulic fluid in the strut. This control loop is toggled on and off during an experiment. Data shown in figure 8 had the acceleration feedback loop turned on after 14 seconds. The upper mass position is reduced to 25 % of the uncontrolled position after the axle load feedback loop is turned on. Drift after the initiation of control in the stroke and upper mass position histories in figure 8 could be attributed, in part, to a continuous decrease in the control system hydraulic supply pressure. All simulation results assume a constant control system hydraulic supply pressure. To experimentally minimize the effect of reduced control system hydraulic supply pressure, long duration tests were interrupted periodically to allow for the recovery of system hydraulic pressure. Discrepancies in stroke levels between test and simulation are not well understood.

Friction played a key role in unrestrained tests performed with this testbed. To illustrate the problem, figure 9 shows a frequency response function of the upper accelerometer to servo command. Note that the landing gear locks-up above 0.7 Hz due to friction. Control authority is lost beyond 0.7 Hz due to high friction levels, about 2000 lbf. statically and 400 lbf. dynamically. This static friction level causes a condition in which pressure versus stroke equilibrium can be in error by as much as plus or minus 45 psi. Also important is the use of nitrogen in the upper chamber. Nitrogen serves as a soft cushion for load transfer through the landing gear. In the absence of nitrogen the strut is full of hydraulic fluid, which is incompressible, and therefore small amounts of hydraulic fluid into or out of the strut causes large changes in the internal pressures. Since the servo hydraulic has a limited supply of external hydraulic fluid, the absence of nitrogen allows for longer test time and higher forces in the system but requires higher pressures for the external supply.

Controlled tests like the one shown in figure 8 can only be performed at discrete frequencies with the capabilities of the existing hydraulic system. To test the frequency range between 0.1 Hz to 4 Hz, a spectrum analyzer was set for a sine-sweep and the test was conducted over a long period of time, stopping periodically to allow for the hydraulic system to be re-supplied. Open and closed-loop results from this test

are shown in figure 10. Note that in this test the shaker table was used as the input disturbance and provided enough energy to prevent the system from locking up below 1.2 Hz. Feedback from position and axle load signals were used in the control system to attenuate responses between 1.5 and 3.5 Hz. The maximum amplitude reduction is a factor of 4.4 at 1.4 Hz with reductions beyond 3.5 Hz of about 20%. Using the strain gage sensor to measure axle load provides a cleaner signal for feedback and reduces the risk of high frequency instabilities in the feedback loop. Note that in the ideal case with the control system fully charged, a gain optimized for a single frequency, and controlling the system at its natural frequency, amplitude reductions of a factor of 10 have been observed.

6. Summary

Equations of motion for a telescoping landing gear system have been developed incorporating an external servo-hydraulic system which allows for landing gear actuation. The electronic servo hydraulic system model combined the electronic and hydraulic dynamics in one relatively simple formulation. A number of aspects of actively controlled landing gear design have been demonstrated in this study. Fuselage vibration reduction levels by a factor of 4 have been demonstrated along with some of the fundamental limitations of implementing such systems in landing gear design. High friction levels hindered the ability to achieve higher performance without a major re-design of the landing gear. However, even modest vibration reductions may translate into reductions in landing gear loads and therefore aircraft structural weight.

References

1. Currey N.S.: *Aircraft Landing Gear Design: Principles and Practices*. AIAA Education Series, 1988.
2. Milwitzky, B.; and Cook F.E.: Analysis of Landing-Gear Behavior. NACA Report No. 1154, 1953.
3. Ottens, H.H.: Predicted and Measured Landing Gear Loads for the NF-5 Aircraft Taxiing over a Bumpy Runway. AGARD-CP 326, 1982.
4. Payne, B.W.; Dudman A.E.; Morris, B.R.; and Hockenhull, M.: Development of a Cost Effective Approach to Modeling Aircraft Response to Repaired Runways. *Proceedings of the 52nd meeting of the AGARD Structures and Materials Panel*, Cesne, Turkey, April 1981.
5. Freymann R.: An Experimental-Analytical Routine for the Dynamic Qualification of Aircraft Operating on Rough Runway Surfaces. AGARD R-731, March 1987.
6. Gerardi T.G.; and Ninnetyan L.: Status of Computer Simulations of USAF Aircraft and an Alternative Simulation Technique. AGARD CP-326, April 1982.
7. Freymann R.; and Johnson W.: Simulation of Aircraft Taxi Testing on the AGILE Shaker Test Facility. *Second International Symposium on Aeroelasticity and Structural Dynamics*, sponsored by Deutsche Gesellschaft fur Luft- und Raumfahrt e.V. in Aachen, W. Germany, April 1985.
8. Sheperd A.; Catt T.; and Cowling D.: The Simulation of Aircraft Landing Gear Dynamics. *18th Congress of the International Council of the Aeronautical Sciences*, Beijing, People's Republic of China, Sept. 1992.
9. Catt T.; Cowling D.; and Sheperd A.: Active Landing Gear Control for Improved Ride Quality During Ground Roll. AGARD Smart Structures for Aircraft and Spacecraft, Oct. 1992.
10. Ross I.; and Edson R.: An Electronic Control for an Electro-hydraulic Active Control Aircraft Landing Gear. NASA CR 3113, April 1979.
11. Ross I.; and Edson R.: An Electronic Control for an Electro-hydraulic Active Control Landing Gear for the F-4 Aircraft. NASA CR 3552, April 1982.

12. Freymann R.: Actively Damped Landing Gear System. AGARD CP-484, 1990.
13. Daniels, J.N.: A Method for Landing Gear Modeling and Simulation with Experimental Validation. NASA Contractor Report 201601, June 1996.
14. Horta, L.G.: Daugherty, R.H.: and Martinson, V.J: " Modeling and Validation of an A6-Intruder Actively Controlled Landing Gear System," NASA TP-1999-209124
15. Matlab/simulink User's manual, *Using Simulink, Version 2.0,* The Mathworks, Inc, Natick, MA, 1997

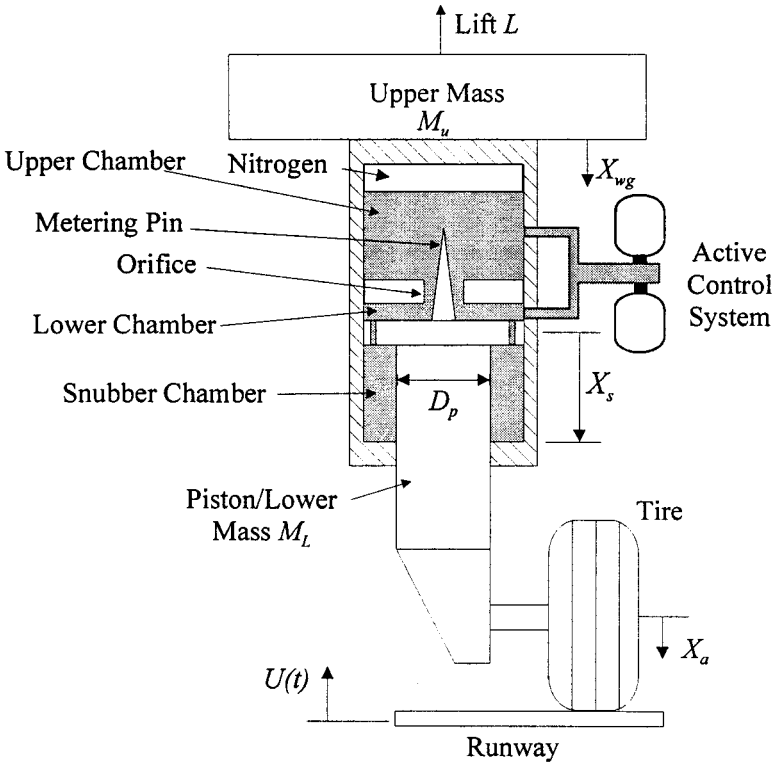

Figure 1. Schematic of a telescoping landing gear

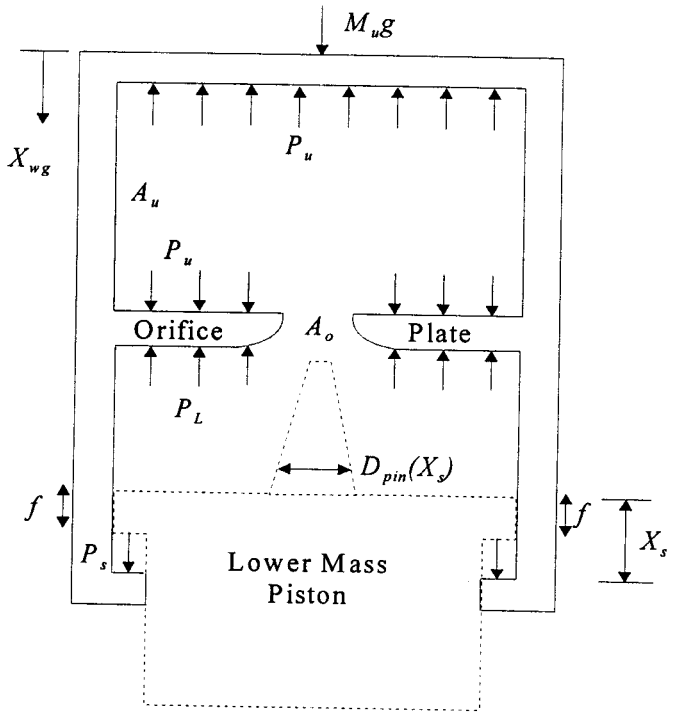

Figure 2. Schematic of upper mass and main cylinder.

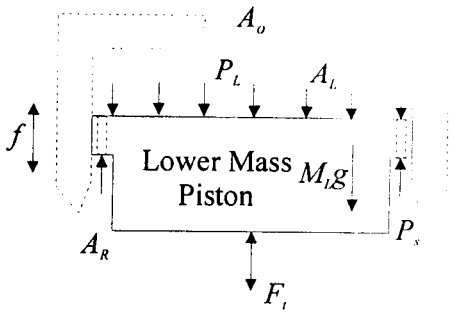

Figure 3. Schematic of lower mass.

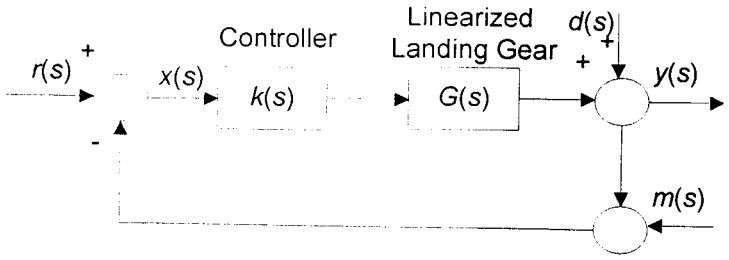

Figure 4. Block diagram of control system.

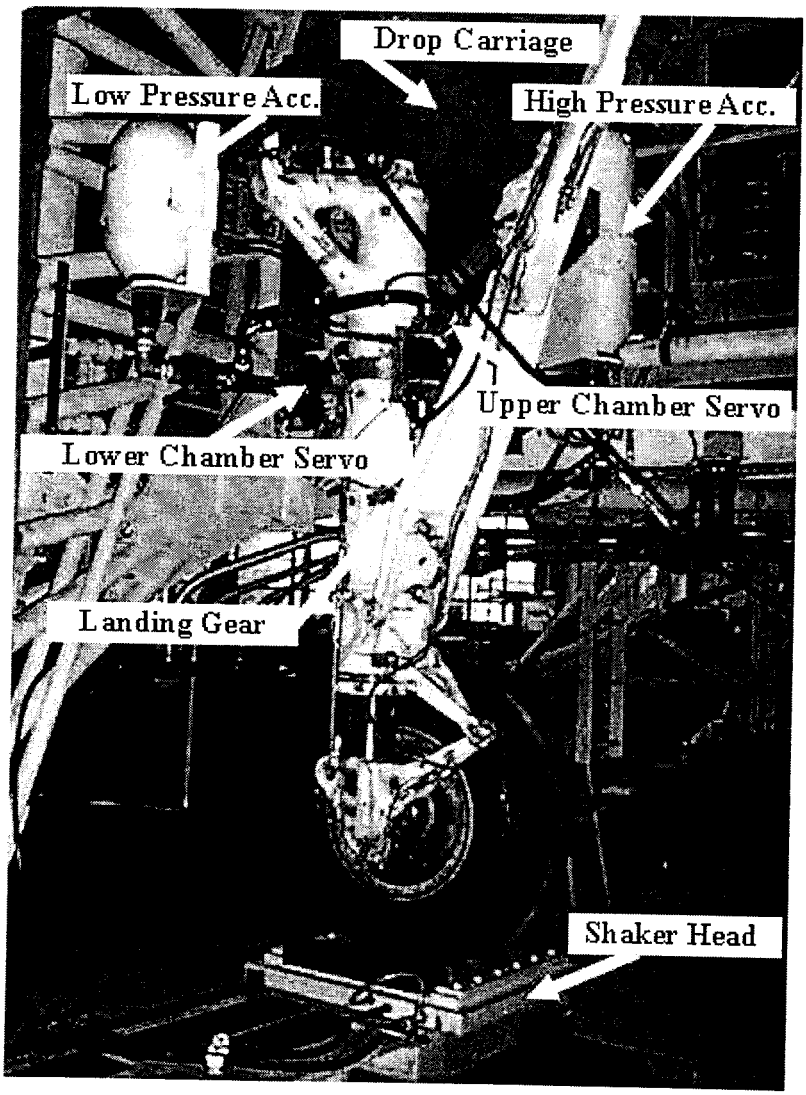

Figure 5. Test set-up for validation of analysis model and control system.

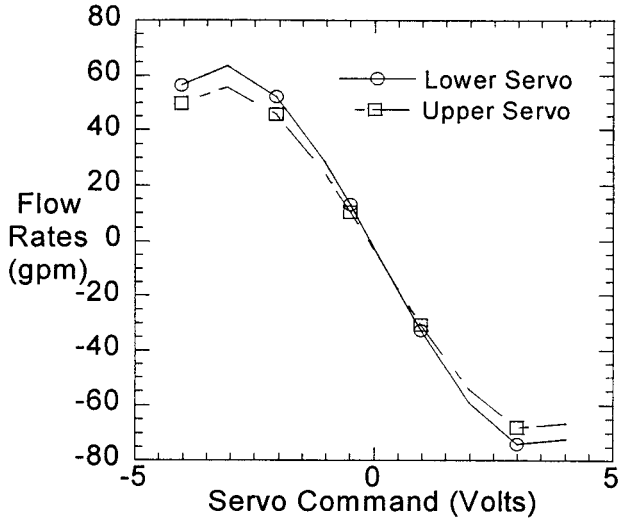

Figure 6. Flow rate as a function of servo commands with unrestrained landing gear and no nitrogen.

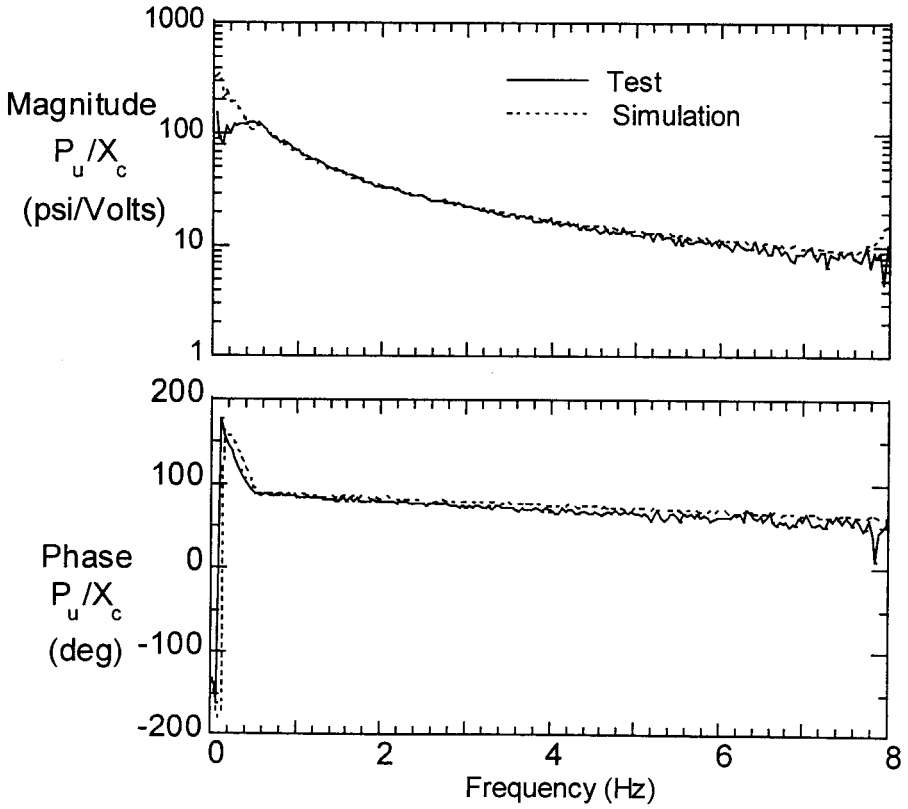

Figure 7. Upper chamber pressure to servo command transfer function.

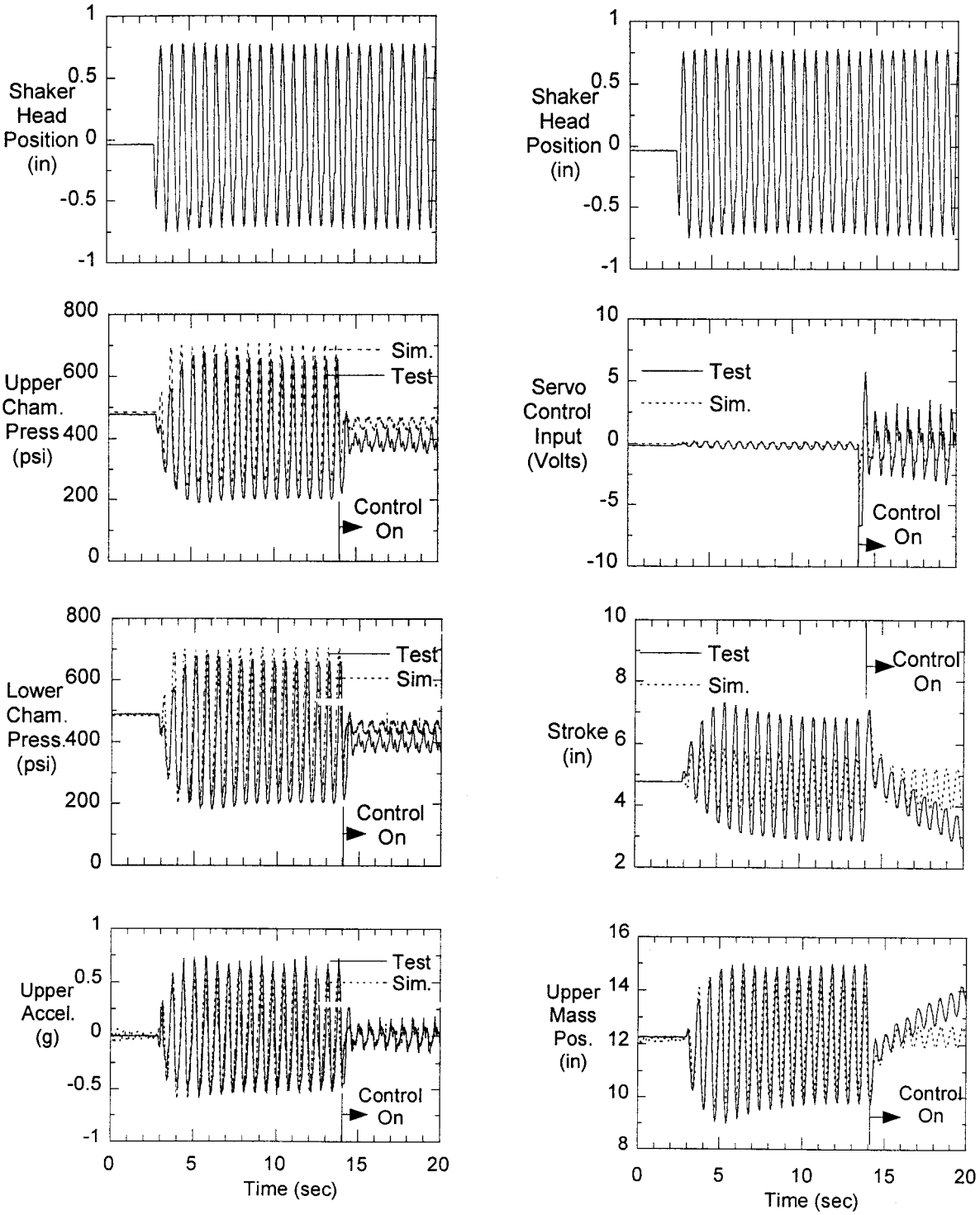

Figure 8. Controlled test and analysis results due to a periodic disturbance at 1.5 Hz.

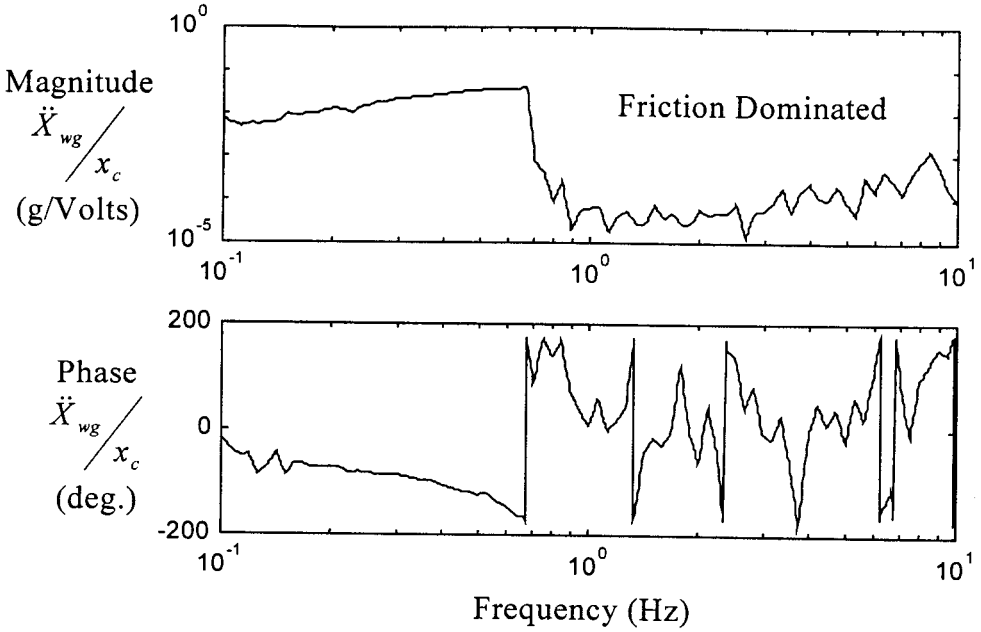

Figure 9. Frequency response from upper servo command to upper accelerometer.

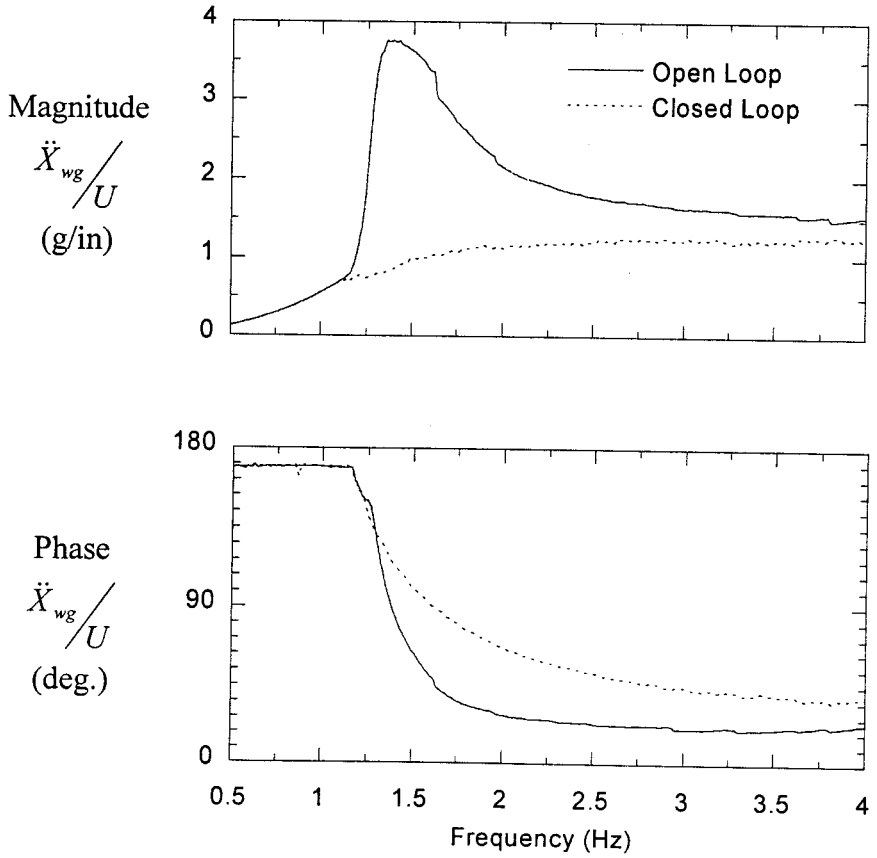

Figure 10. Upper acceleration to shaker position transfer function.